Co-funded by the European Union

Project funded by
Schweizerische Eidgenossenschaft
Confédération suisse
Confederazione Svizzera
Confederaziun svizra
Swiss Confederation
Federal Department of Economic Affairs, Education and Research EAER
State Secretariat for Education, Research and Innovation SERI

# Deliverable 2.1

## Mechanical load profiles

**NKT**

**Andreas Tyrberg,**
**Alessio Rubini,**
**Nikolaos Psichogios,**
**Angelica Chisté**

21.10.2025


# Deliverable 2.1

## Mechanical load profiles

NKT

Andreas Tyrberg,
Alessio Rubini,
Nikolaos Psichogios,
Angelica Chisté

Co-funded by the European Union

Project funded by

# Document General Information

| | |
|---|---|
| **Project Title** | accelerating DC DYNAMIC cable technology for sustainable European electricity grid |
| **Project Acronym** | DCDYNAMIC |
| **Call Topic ID Code** | HORIZON-CL5-2024-D3-01-15 |
| **Grant Agreement** | 101172817 |
| **Project Coordinator** | Dr. Chen, UNIMAN |
| **Deliverable ID** | D2.1 |
| **Delivery Beneficiary** | NKT HV Cables AB |
| **Work Package Number** | 2 |
| **Task Number** | T2.5 |
| **Due Date** | 31 October 2025 |
| **Actual Submission Date** | 23 October 2025 |
| **Project Start Date** | 1 November 2024 |
| **Project Duration** | 48 months |
| **Deliverable Type** | R |
| **Dissemination Level** | PU |

# Version Control

| Issue | Date | Comment | Author(s) |
|---|---|---|---|
| **V0.1** | **10-10-2025** | **Initial version** | **Andreas Tyrberg, Alessio Rubini, Nikolaos Psichogios, Angelica Chisté (NKT)** |
| **V0.2** | **14-10-2025** | **Feedback** | **David Liney (SHELL)<br>Chloe Loveless (UNIMAN)** |
| **V0.3** | **21-10-2025** | **Final version** | **Andreas Tyrberg, Alessio Rubini, Nikolaos Psichogios, Angelica Chisté (NKT)** |
| | | | |

# Table of Contents

# 1 Glossary

| Abbreviation / acronym | Description |
|---|---|
| ALS | Accidental Limit State |
| BS | Bend Stiffener |
| DFF | Design Fatigue Factor |
| FLS | Fatigue Limit State |
| FOSS | Floating Offshore SubStation |
| HVDC | High-Voltage Direct Current |
| MSL | Mean Sea Level |
| RAO | Response Amplitude Operator |
| YRP | Year Return Period |
| ULS | Ultimate Limit State |
| TDZ | Touch Down Zone |

# 2 Executive Summary

This report outlines the mechanical load profiles of a high voltage direct current dynamic cable developed within the framework of the DCDYNAMIC project.
The document begins by presenting the design basis, including the selection of the cross section for the high-voltage direct current (HVDC) cable, the identification of a technically and operationally feasible cable configuration, and a description of the platform and the met-ocean data. For the purpose of this study, an existing concept of floating substation developed by Aibel AS and Hitachi Energy, with an export cable, is selected. The platform is located in the North Sea, and the corresponding environmental conditions are applied to the analysis.
The report then describes the global analysis methodology, including the selection of load cases and acceptance criteria. The global analysis studies the cable system under various environmental scenarios including the influence of the platform motions. It accounts for all relevant static and dynamic loads present in the offshore environment and evaluates the cable´s response in the time domain.
The results section covers the cable configurations, the outputs of the extreme and fatigue analyses, and concludes with the evaluation of strain in the cable insulation. The extreme analysis confirms that the lazy and tether wave configurations are viable candidates for the project for the offshore environmental conditions under consideration, as they meet the acceptance criteria. In contrast, the results demonstrate that a free-hanging configuration will require special considerations in order to be feasible with respect to touchdown zone dynamics. Additionally, the fatigue analysis demonstrates that the cable's lifetime requirements are fulfilled.
The outputs of the global analysis enable a detailed assessment of the strain within the conductor insulation, which represents a critical aspect of the project. Strain is evaluated in the insulation of the cable and for multiple configurations.
A full fatigue analysis is performed to study the fatigue loading of the insulation during 30 years of operation and the result from the simulation study is presented in the form of histograms showing the strain range vs. expected number of cycles. It has been found that the largest dynamic strain ranges experienced by the insulation system during fatigue loading are less than 0.4%. The maximum dynamic strain range seen during an extreme event corresponding to 100 YRP condition is 1.4%. These results will serve as input for the experimental testing that is planned within DCDYNAMIC for which it is important to establish realistic and relevant strains representative for fatigue loads experienced by a dynamic HVDC export cable.

# 3 Introduction

As global energy demand continues to rise, the need for innovative and cost-efficient energy solutions is becoming increasingly critical to achieve net-zero greenhouse gas emissions by 2050. The wind industry is evolving quickly, with offshore wind expected to play a key role in its expansion, which will drive increased demand for export cable capacity. Special focus should be placed on floating wind technology, providing access to greater depth and higher wind speed.

One of the major challenges in offshore energy production is the efficient transmission of power from offshore platforms to onshore grids. High-voltage direct current (HVDC) cables offer the best solution to minimize transmission losses in remote locations. However, no dynamic HVDC cables have been installed so far, making the transition to floating wind even more complex.

The DCDYNAMIC project addresses this challenge by focusing on the insulation system of a dynamic HVDC export cable. The project investigates insulation aging, the electro-mechanical-thermal behaviour of the cable and includes laboratory testing of a 320 kV prototype. This Deliverable 2.1 examines the cable´s mechanical loads during extreme and fatigue analysis conditions. The study is based on an existing concept of a floating HVDC converter connected to the export cable, located in the harsh environment of the North Sea.

To accurately assess the real-world conditions affecting the platform and cable, a global dynamic analysis is essential. The main objectives are to determine the extreme and fatigue loads experienced during cable´s design life. First, a suitable cable cross-section and configuration are defined. The results of the global analysis are then used to calculate strain in the cable's insulation through detailed cross-sectional analysis. The global analysis is performed using OrcaFlex from Orcina, a 3D simulation software that models the global configuration and computes tension and curvature along the cable's entire length. The cross-sectional analysis is performed using Helica from DNV and literature.

The final strain observed in the cable's insulation is representative of the mechanical fatigue loading and will serve as a reference for laboratory validation testing in Work Package (WP) 5. It will be used also for WP1 andWP2 to understand representative strain variations seen by a dynamic HVDC cable during operation.

# 4 Design Basis

## 4.1 System of Units

The units follow the SI system.

## 4.2 Design Life

The design fatigue life is assumed to be 30 years, which is a typical requirement specified for dynamic cables.

## 4.3 Platform Description, Floating Platform

### 4.3.1 Platform Particulars

The analysis considers an existing concept of floating platform in the North Sea. It is a floating platform concept developed by Aibel AS and Hitachi Energy for a ±320 kV HVDC converter station: 1.4 GW ±320kV HVDC FOSS. Its displacement RAOs are used in the study, provided for 23 directions. Figure 1 and Figure 2 show the floating platform.

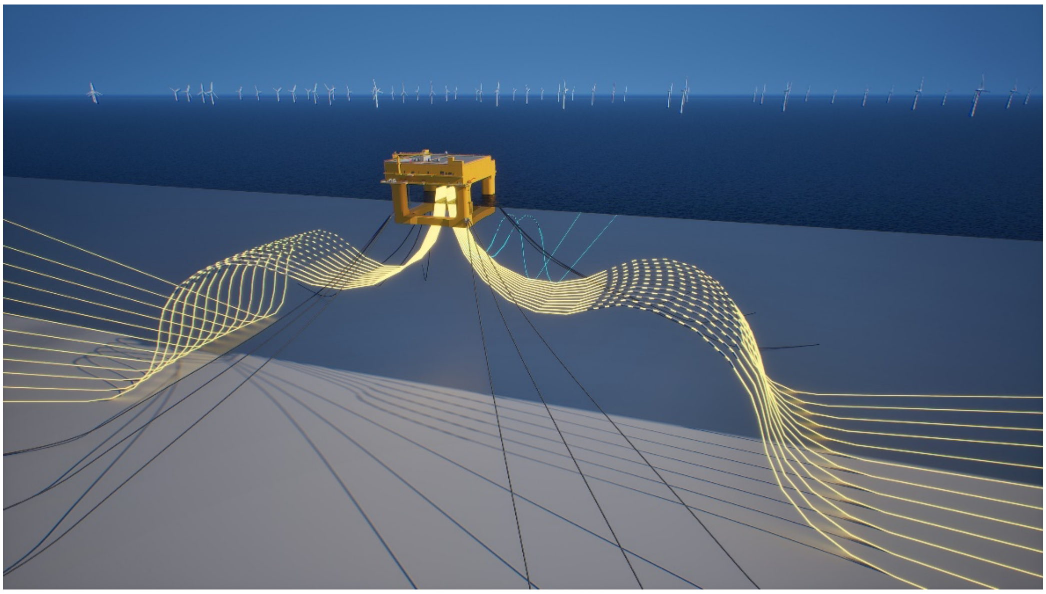

*Figure 1: Floating platform with HVDC converter. Courtesy of Aibel AS and Hitachi Energy*

*Figure 2: Zoomed-In view of floating platform with HVDC converter. Courtesy of Aibel AS and Hitachi Energy*

### 4.3.2 Coordinate System

The platform centre of coordinate is located at the geometrical centre and on the keel-level (22 m below MSL). The x-axis is positive towards East, the y-axis is positive towards North and z-axis is positive up. Figure 3 shows the x-y axis and Figure 4 shows the x-z axis of the platform's coordinate system.

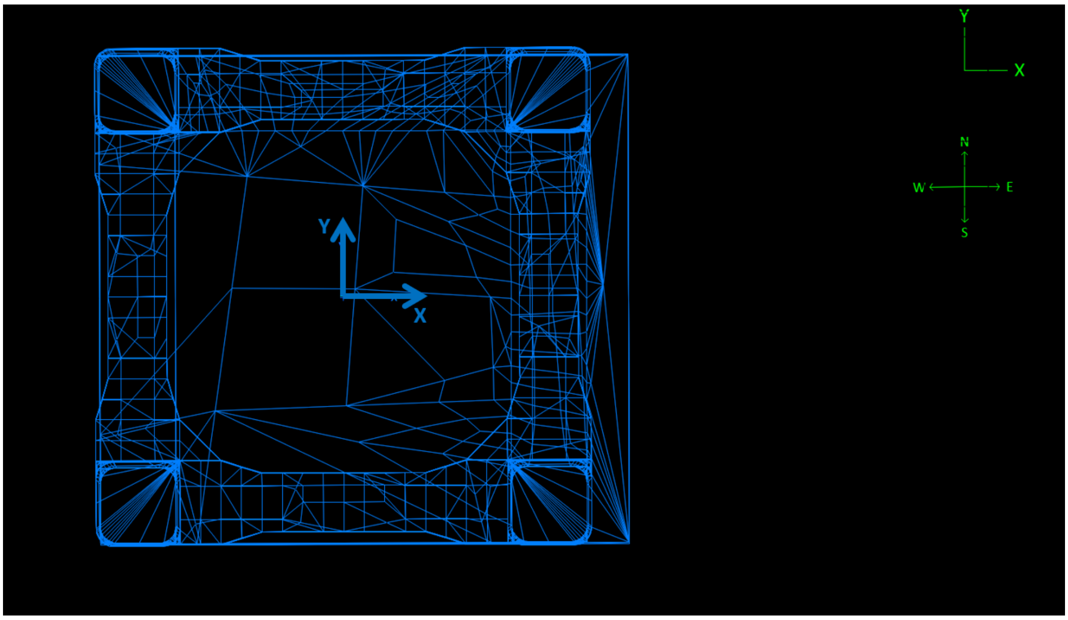


*Figure 3: Platform coordinate system: x-y*

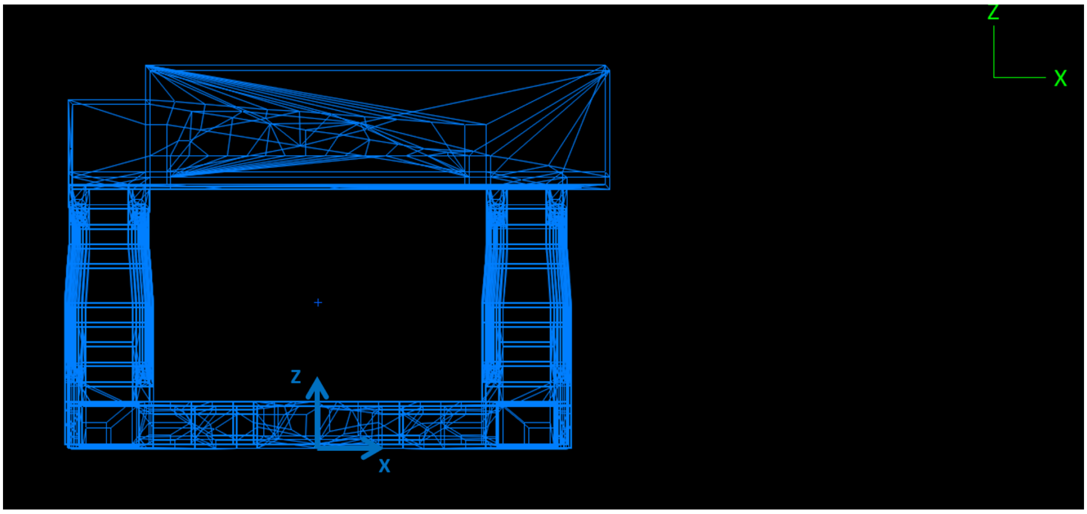


*Figure 4: Platform coordinate system: x-z*

### 4.3.3 Hang-off Location

The hang-off is located in the north-west part of the platform as starting point, presented in Table 1 and Figure 5.

*Table 1: Hang-off location in platform coordinate system*

| X | Y | Z |
|---|---|---|
| -5.55 m | 2.25 m | 39.5 m |

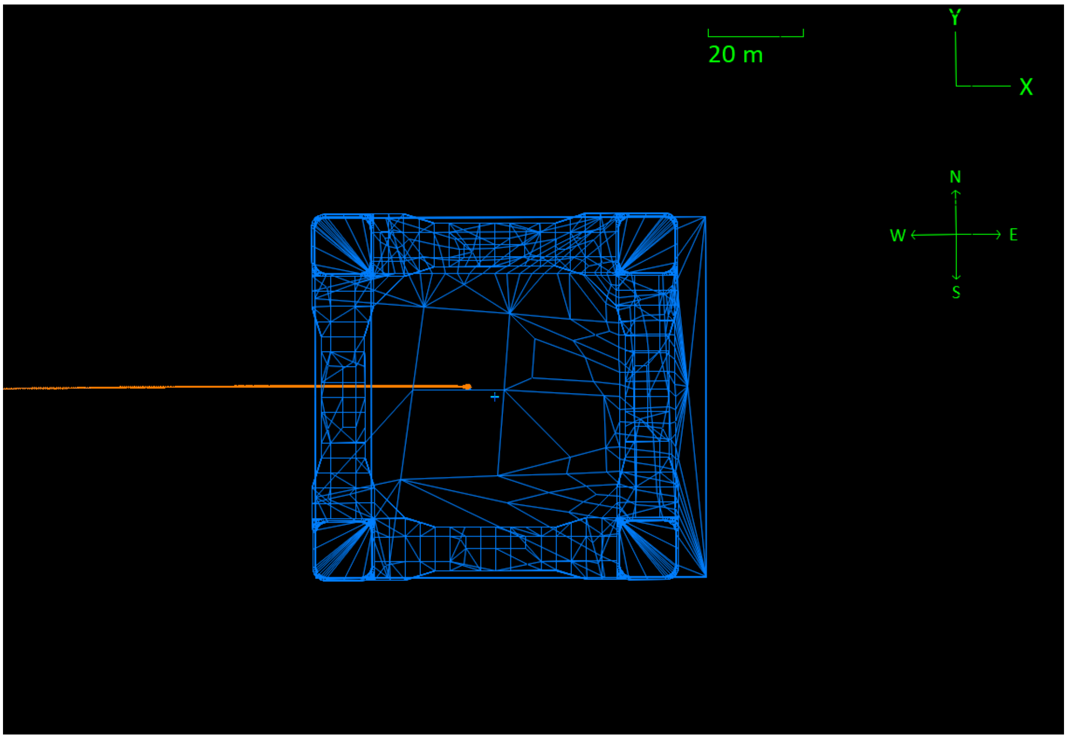


*Figure 5: Hang-off location for the export cable*

### 4.3.4 Offsets

Realistic maximum omni-directional offsets of the platform are provided, as presented in

Table 2, and a linear interpolation based on the water depth is applied.

*Table 2: Maximum omni-directional offsets of the platform*

| Limit State Condition | Water depth 200 m | Water depth 400 m | Water depth 1000 m |
|---|---|---|---|
| ULS 100 yr | 59 m | 74 m | 186 m |
| ALS 100 yr + 1 Line Broken | 88 m | 108 m | 201 m |

## 4.4 Dynamic Export Cable Properties, HVDC 320 kV

The export cable proposed for the DCDYNAMIC project is a 320 kV DC double armoured - three core cable design with a power transmission capacity of 1 GW. The cross-section is based on 1700 $mm^2$ copper conductors, XLPE insulation and corrugated sheaths.

Table 3 presents the main mechanical properties of the dynamic cable.

*Table 3: Nominal mechanical properties of the 3x1700 $mm^2$ dynamic cable*

| Item | Unit | Value |
|---|---|---|
| Outer diameter | mm | 295 |
| Dry weight | kg/m | 150 |
| Wet weight, approx. | kg/m | 93 |

Linear post slip bending stiffness of the cable is used in the analysis as an assumption, for a conservative result.

## 4.5 Dynamic Cable Configuration

Three different configurations are analysed in the global analysis to identify which scenarios are feasible and the level of strain in insulation for each scenario: free-hanging, lazy wave and tether wave configurations.
A detailed drawing and data of the floating platform are used in OrcaFlex to represent the platform. The HVDC dynamic cable is added to the model. The proposed dynamic cable has its hang-off point 17.5 metres above Mean Sea Level (MSL) in all configurations.

The free-hanging configuration, Figure 6, presents a single cable extending from the platform to the seabed. It is the most cost-effective configuration.

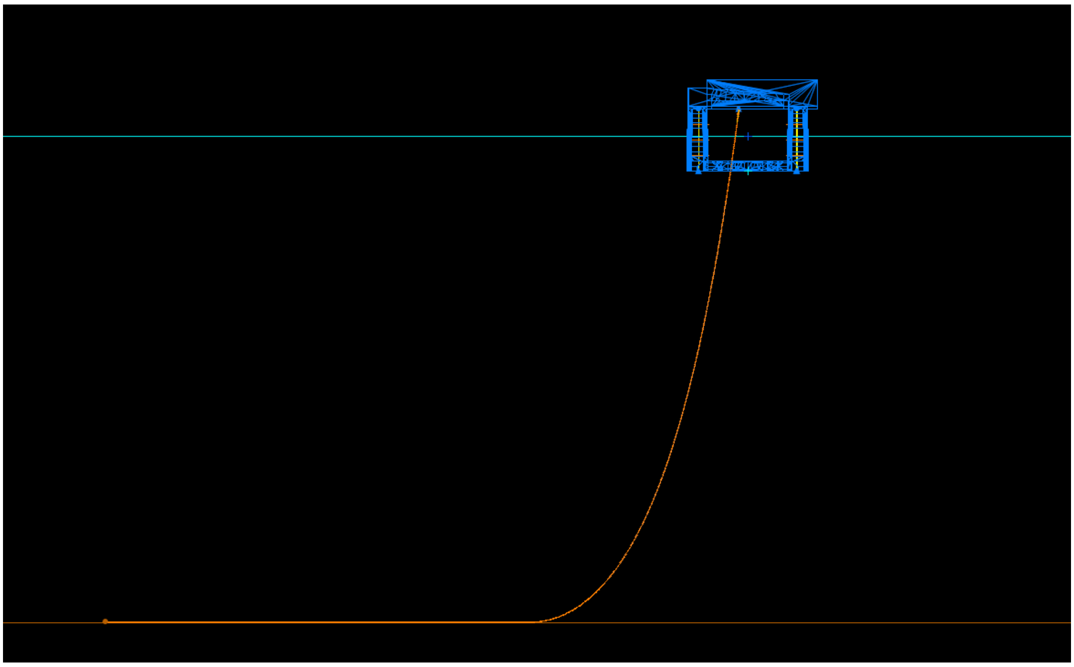

*Figure 6: Side view of free-hanging configuration*

The lazy wave configuration, Figure 7, resembles the free-hanging configuration but it has buoyancy modules that provide the necessary upthrust to maintain the desired cable profile.

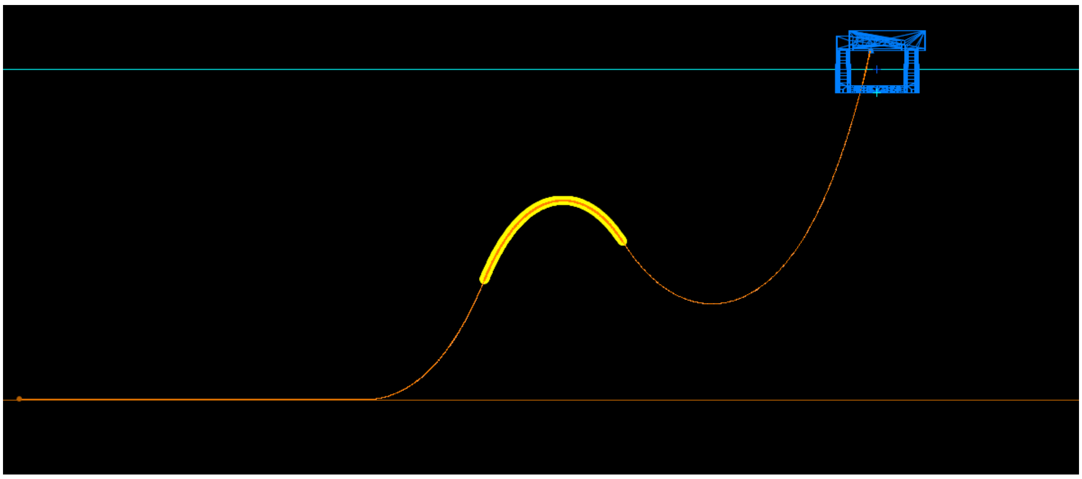

*Figure 7: Side view of lazy wave configuration*

The tether wave configuration, Figure 8, is similar to the lazy wave with the addition of a hold down system that provides downward tension and restrains the touchdown point.

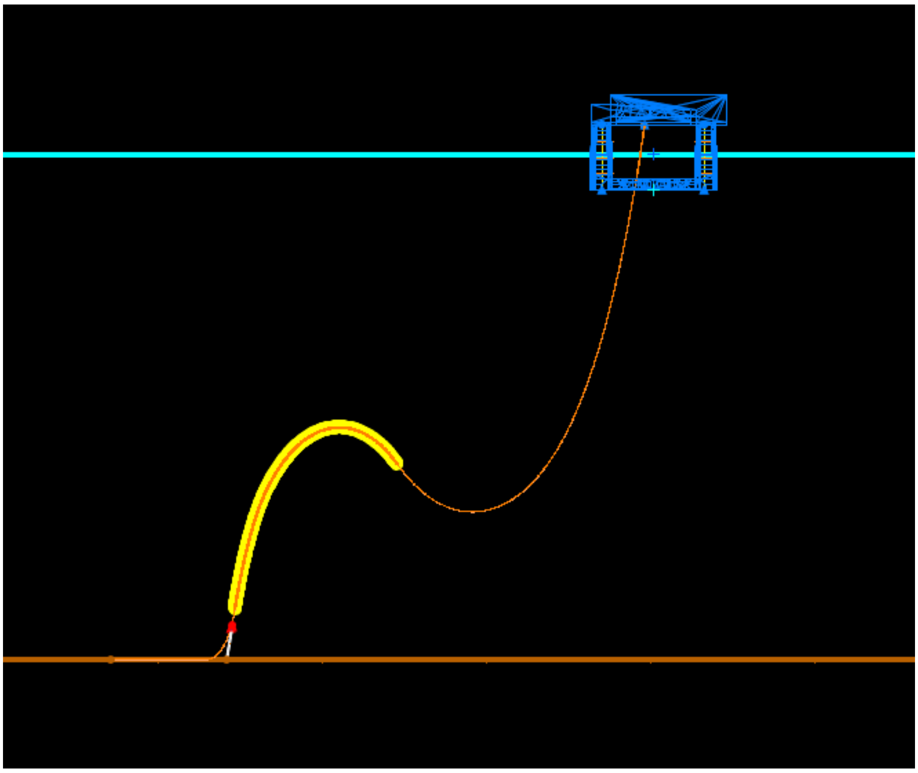

*Figure 8: Side view of tether wave configuration*

A free-hanging configuration is first investigated as the starting point.

### 4.5.1 Bend Stiffener

The bend stiffener (BS) protects the cables against excessive bending near the hang-off location. Its design requires thermal, dynamic and structural analyses, making the process iterative.
A scaled bend stiffener is used as starting point with a built-in angle of 7 degrees relative to vertical. The temperature of the BS is assumed to be 40 °C for conservative results. Figure 9 presents the BS radius along the length.

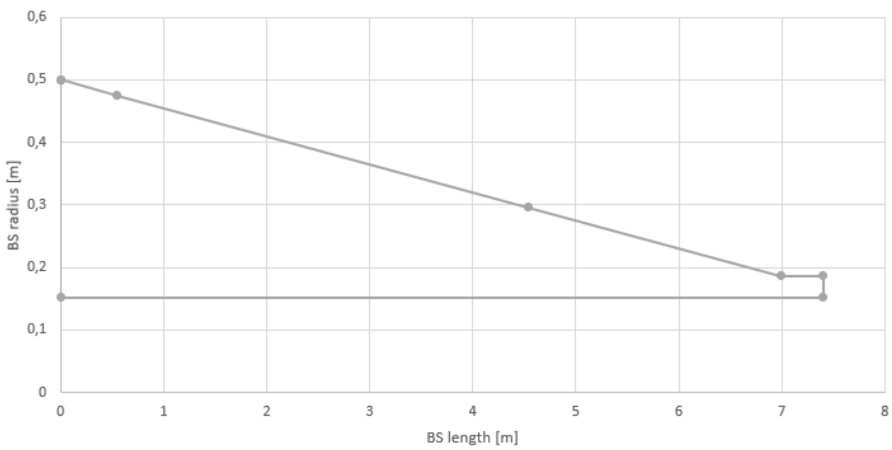


*Figure 9: Bend stiffener radius and length*

### 4.5.2 Buoyancy Modules

The buoyancy modules provide upthrust to support both lazy wave and tether wave configurations.
As a starting point, the buoyancy modules have the design presented in Table 4.

*Table 4: Preliminary buoyancy modules properties*

| Buoyancy modules | Unit | Value |
|---|---|---|
| Length | m | 1.3 |
| Outer Diameter | m | 1.3 |
| Module net buoyancy, nominal | kg | 827.5 |

The buoyancy modules and the cable are modelled with equivalent uniform properties, having equivalent mass, amount of buoyancy, normal drag area and tangential drag area of the single buoyancy modules and the cable.

## 4.6 Met-Ocean Conditions

### 4.6.1 Introduction – North Sea

The platform is located in the North Sea with a water depth of 308 metres. The met-ocean environment is based on actual data for a representative site in the North Sea and it considers various waves and currents for various directions.

### 4.6.2 Waves and Current

Extreme directional wave and current data are available for 12 directions. Return periods of 1, 10, 100 years are considered. All wave heights are studied for three different periods.
Table 5 presents the characteristics of omni-directional, 100 year return period (YRP) waves.

*Table 5: Omni-directional wave characteristics, 100 YRP*

| Hs | Tp, P5 | Tp, P50 | Tp, P95 | Hmax | T, P5 | T, P50 | T, P95 |
|---|---|---|---|---|---|---|---|
| 15.9 m | 15.0 s | 17.3 s | 19.8 s | 29.7 m | 13.5 s | 15.6 s | 17.8 s |

Table 6 presents the speed of omni-directional 100 YRP current for different water depths.

*Table 6: Omni-directional current speed, 100 YRP*

| Depth [m] | 0 | 30 | 50 | 70 | 100 | 150 | 250 |
|---|---|---|---|---|---|---|---|
| Speed [m/s] | 1.25 | 1.16 | 1.05 | 1.04 | 0.95 | 0.91 | 0.70 |

An omni-directional regular wave scatter diagram corresponding to a 100 year return period is used, in combination with the associated wave sector probabilities.

Regular omni-directional waves ($5^{th}$ order Stokes′ theory) and collinear wave-current are studied.

### 4.6.3 Marine Growth

The marine growth affects the outside diameter, the volume and, the mass of the cable and buoyancy modules. The thickness and density of marine growth is based on the standard NORSOK N-003 [1] and are a function of the water depth. Table 7 presents the marine growth as a function of the water depth.

*Table 7: Thickness and density of marine growth*

| Depth [m] above MWL | Thickness [mm] | Density [kg/m$^3$] |
|---|---|---|
| +2 | 0 | - |
| -15 to +2 | 60 | 1325 |
| -30 to -15 | 50 | 1325 |
| -40 to -30 | 40 | 1325 |
| -60 to -40 | 30 | 1100 |
| -100 to -60 | 20 | 1100 |
| Below -100 | 10 | 1100 |

# 5 Global Analysis

The global analysis of the dynamic cable system considers the Aibel AS and Hitachi Energy 1.4 GW ±320kV HVDC FOSS and the environmental conditions. The main outputs of the global analysis are the static and dynamic loads of the cable in the time domain. Both extreme and fatigue analyses are studied. The loads are calculated for three different configurations, see Chapter 4.

## 5.1 Software

The extreme and fatigue global analyses are performed in OrcaFlex from Orcina, using Python for the pre- and post-processing analyses.
OrcaFlex is a 3D, non-linear solver based on discrete elements and multi-bodies. It provides time and frequency domain solutions.
The local analysis is performed in Helica, developed by DNV, a software for cross-sectional analysis of flexible pipes and umbilicals.

## 5.2 Methodology

The analysis is performed in the time domain, incorporating displacement RAOs of the floating substation associated with maximum vessel offsets. The base case scenario considers regular waves conditions, representative of typical offshore environments.
Three different configurations are studied to identify feasible scenarios and the resulting maximum strain response. Both extreme and fatigue load cases are simulated. The fatigue analysis is studied for three directions considering merged probabilities. It specifically studies critical regions of the cable, including the bend stiffener and sag-hog zones, where the curvature variations, and therefore the strain variations in the insulations, are expected to be the largest. The strain in the insulation is calculated through local analysis, based on both literature and Helica simulations.

## 5.3 Selected Load Cases

The analysis considers various load cases, each representing different environmental conditions and platform scenarios. The selection of these load cases, presented in Table 8, is based on both requirements and insights gained from previous studies conducted in the same geographical area. This approach ensures that the analysis captures realistic conditions, allowing for a representative calculation of the mechanical loads.

*Table 8: Load case matrix*

| Load Class | Scenario | Wave | Current | Directions | System State | Offset Scenarios |
|---|---|---|---|---|---|---|
| ULS | Extreme conditions | 100 y | 10 y | All-collinear | Intact | Max offset, Half offset, 100 y |
| | | 10 y | 100 y | | | |
| ALS | Abnormal conditions | 100 y | 10 y | All-collinear | One broken mooring line | Max offset, Half offset, 100 y |
| | | 10 y | 100 y | | | |
| FLS | Normal operations, fatigue | 100 y scatter | No current | 3 directions | Intact | No offset |

Each load case considers a unique combination of environmental conditions, including various types of waves and current.

- **Load class and Scenario**

To ensure comprehensive coverage of the design scope, the analysis is structured around three main limit states: ultimate, accidental, and fatigue. Extreme and abnormal conditions are considered for the extreme analysis, and normal conditions are considered for the fatigue analysis. A total of 432 load cases are defined for the Ultimate Limit State (ULS) and Accidental Limit State (ALS), while 1203 load cases are considered for the Fatigue Limit State (FLS).

- **Wave and Current**

Waves and current, in this selected load case matrix, are considered collinear and includes 12 different directional sectors. Three directions are used for the fatigue analysis: waves coming from 180, 235, 270 degrees, clockwise from north.

- **System State**

The system state within each load case reflects the condition of the mooring system; specifically, the ALS scenarios account for the failure of one mooring line.

- **Offset Scenario**

The offset scenarios used in the analysis are based on a 100 year return period and include both maximum and half offsets, providing a realistic representation of the platform displacement.

## 5.4 General Acceptance Criteria

The acceptance criteria for the dynamic cables are defined to ensure structural integrity. The main criteria of the extreme and fatigue analysis are:

1. Tension: the analysis verifies that the dynamic cable tension does not exceed its maximum capacity throughout the cable length;
2. Compression: the analysis verifies that the dynamic cable compression does not exceed its maximum capacity throughout the cable length;
3. Bend radius: the analysis verifies that the that the minimum bend radius is respected throughout the cable length, and consequently the maximum curvature;

4. No slack in the hold-down system: the hold-down system in the tether wave configuration must always be in tension;
5. Strain in the BS: the strain in the bend stiffener must be lower than 10%;
6. No interference between the cable and the platform and between the sag-hog segment and the seabed;
7. The design life shall be satisfied with a design fatigue factor (DFF) of 10.

# 6 Results

## 6.1 Cable Configuration

The free-hanging configuration, Figure 10, extends from the hang-off point to the anchor point in the seabed. The cable total length is 639 m, and it has a built-in angle of 7 degrees.

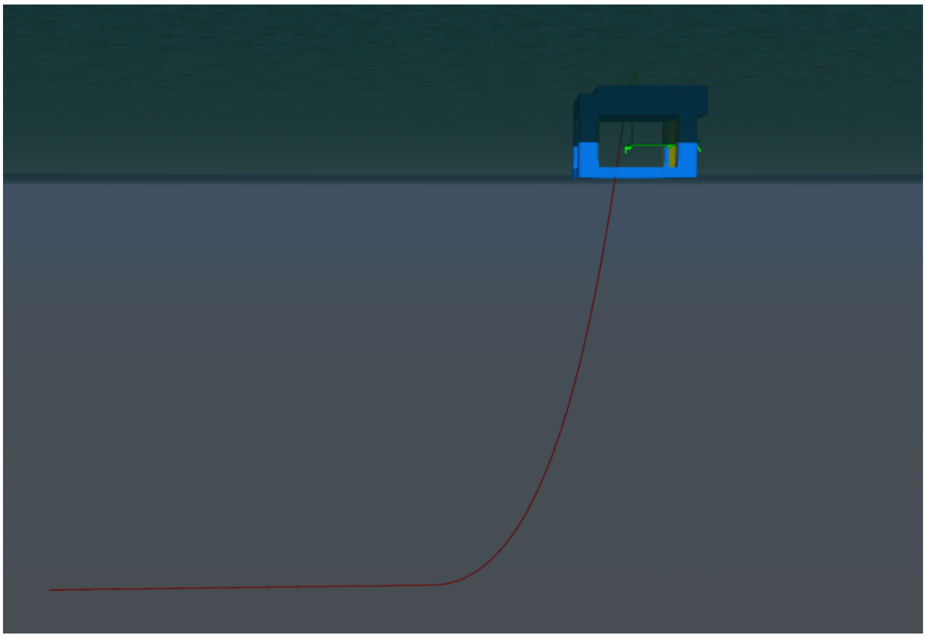

*Figure 10: Side view of free-hanging configuration*

The lazy wave configuration, Figure 11, has a total length of 1072 m, 180 m of buoyancy and a built-in angle of 7 degrees.

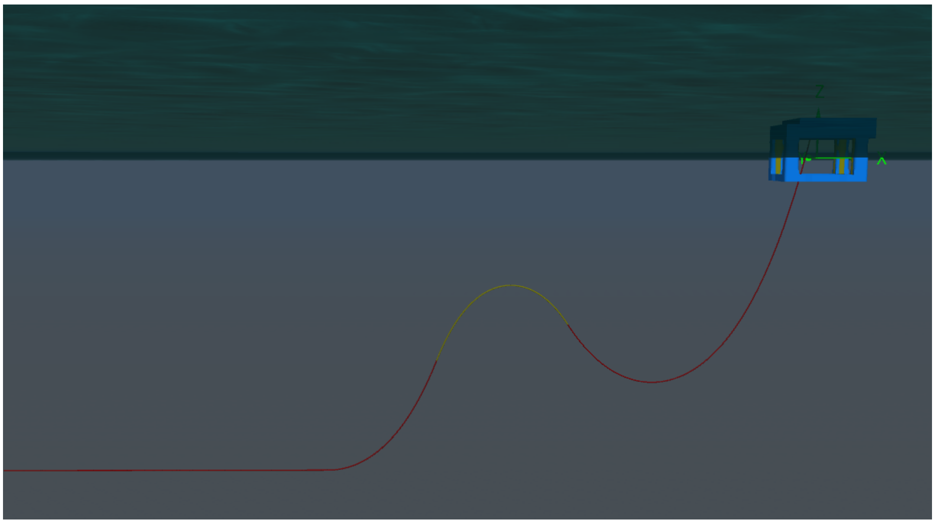

*Figure 11: Side view of lazy wave configuration*

The total length for the tether wave configuration, Figure 12 , is 604 m, with 180 m of buoyancy and with a built-in angle of 7 degrees.

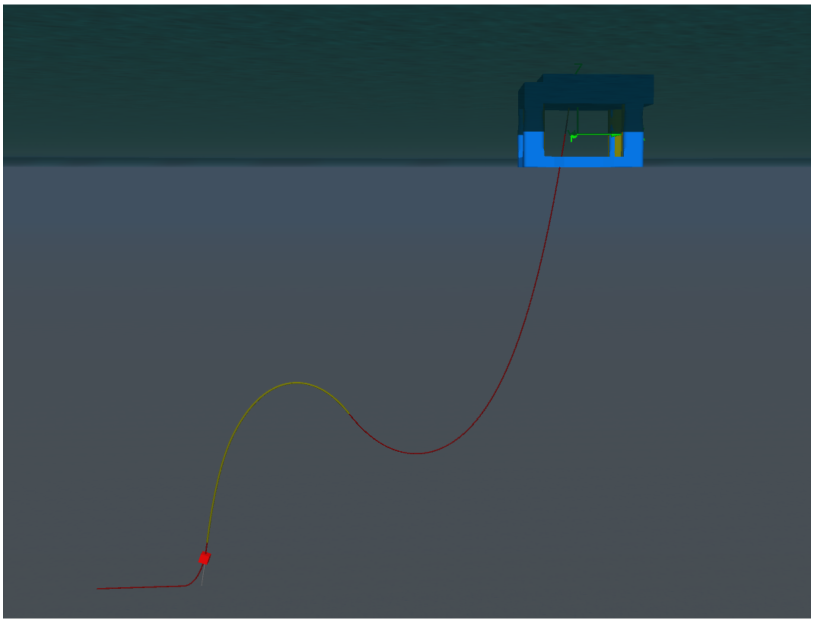

*Figure 12 Side view of tether wave configuration*

## 6.2 Extreme Analysis Results

The free-hanging configuration is analysed and is not found to be fit for purpose under the conditions considered. The results of the extreme load analysis indicate that the compression, the tension capacity and the minimum bend radius requirements of the dynamic cable are not fully met. Particular attention must be given to the touchdown zone, which is a critical area where the cable interacts with the seabed. The free-hanging configuration, given these environmental conditions, platform offsets and cable design, overbends at the touchdown zone, as shown in Figure 13, and exceeds the tension and compression capacity.

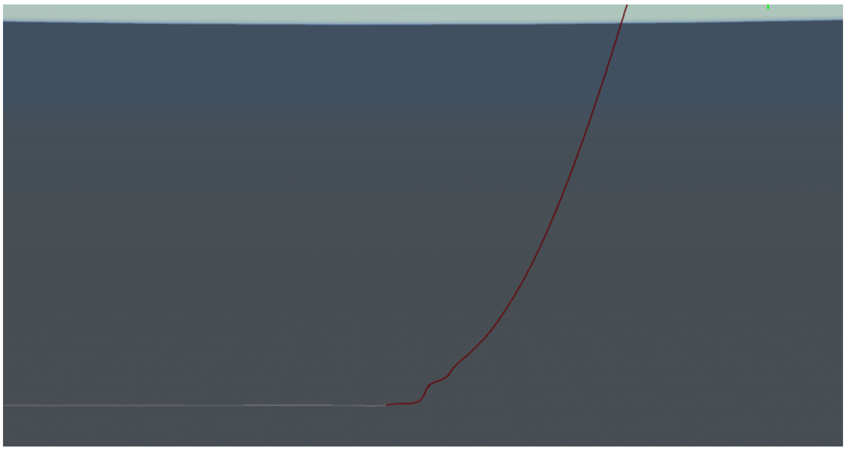

*Figure 13: Overbending in the touch down zone, free-hanging configuration*

Lazy wave configuration is then analysed and Table 9 shows the minimum and maximum effective tension in the cable. In addition, Table 10 shows the bend radius of the cable for a lazy wave configuration.

*Table 9: Effective tension in the lazy wave configuration*

| Effective tension HVDC 320 kV | Minimum [kN] | Maximum [kN] |
|---|---|---|
| Entire length | 4 | 502 |
| TDZ | 6 | 194 |
| BS | - | 502 |

*Table 10: Bend radius in the lazy wave configuration*

| Bend radius | Minimum [m] |
|---|---|
| BS | 11.7 |
| Upper catenary | 35.5 |
| Buoyancy | 22.5 |
| TDZ | 12.0 |
| Seabed | 64.3 |

The tension, compression and bend radius capacities are respected.

The maximum tension of the entire cable, considering all load cases, is in the bend stiffener location, equal to 502 kN. Figure 14 and Figure 15 show the bend stiffener and the entire lazy wave configuration when there is maximum tension in the BS. Specifically in this load case, the wave height is 29.7 m, the wave period is 18.4 s, coming from 270 degrees, clockwise from north.

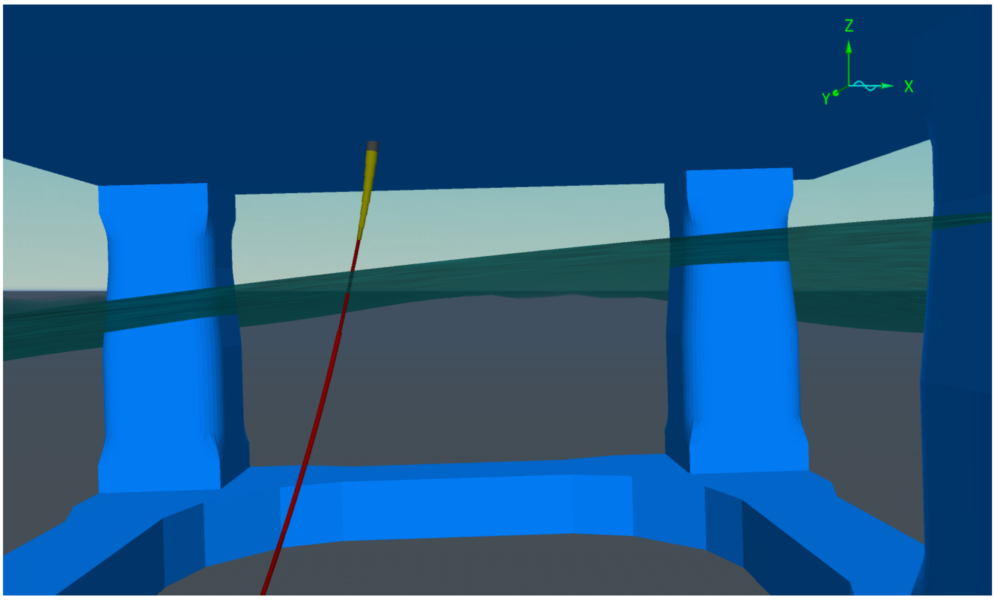


*Figure 14: Bend stiffener in the lazy wave configuration with maximum tension*

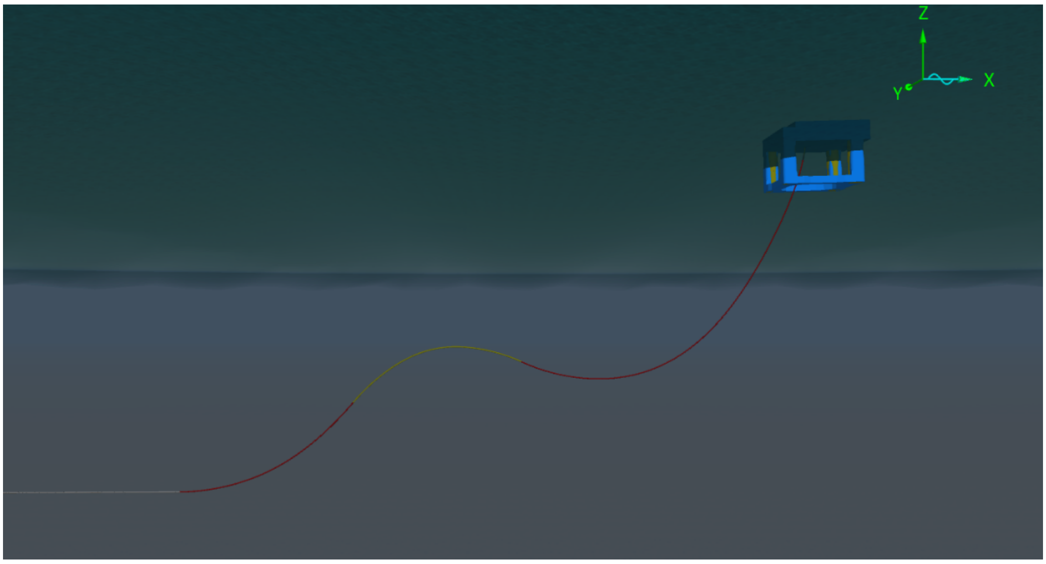


*Figure 15: Lazy wave configuration, max tension in the BS*

Figure 16 shows the lazy wave configuration having the minimum bend radius in the buoyancy segment, considering all load cases. In this specific load case, the wave height is 12.5 m and the wave period 14.7 s, coming from 90 degrees north.

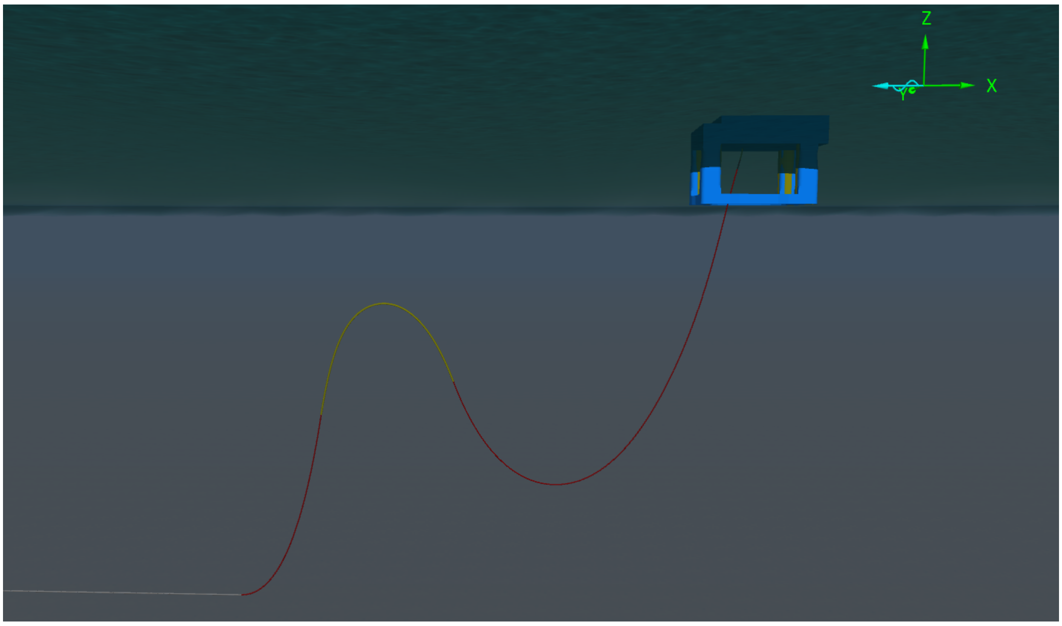


*Figure 16: Lazy wave configuration, minimum bend radius in the buoyancy elements*

Table 11 shows the minimum and maximum effective tension in the cable for a tether wave configuration. In addition, Table 12 shows the bend radius of the cable for different parts for a tether wave configuration.

*Table 11: Effective tension in the tether wave configuration*

| Effective tension HVDC 320 kV | Minimum [kN] | Maximum [kN] |
|---|---|---|
| Entire length | -2 | 471 |
| TDZ | -2 | 61 |
| BS | - | 471 |

*Table 12: Bend radius in the tether wave configuration*

| Bend radius | Minimum [m] |
|---|---|
| BS | 12.6 |
| Upper catenary | 17.5 |
| Buoyancy | 8.7 |
| TDZ | 6.3 |
| Seabed | 27.3 |

The tether wave configuration has the maximum tension in the bend stiffener, presented in Figure 17, equal to 471 kN. In this specific load case, the wave height is 29.7 m and the wave period is 18.4 s, coming from 270 degrees.

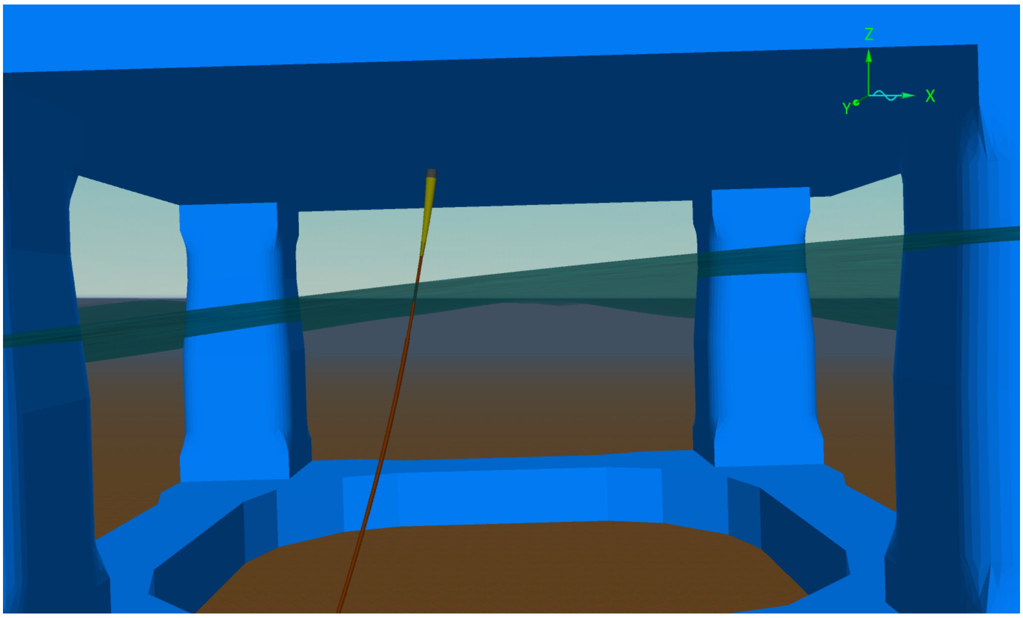


*Figure 17: Bend stiffener in the tether wave configuration with maximum tension*

Figure 18 shows the load case with the minimum bend radius in the buoyancy element part. The wave height is 10.5 m, the wave period 13.9 s and the wave comes from 90 degrees from north clockwise.

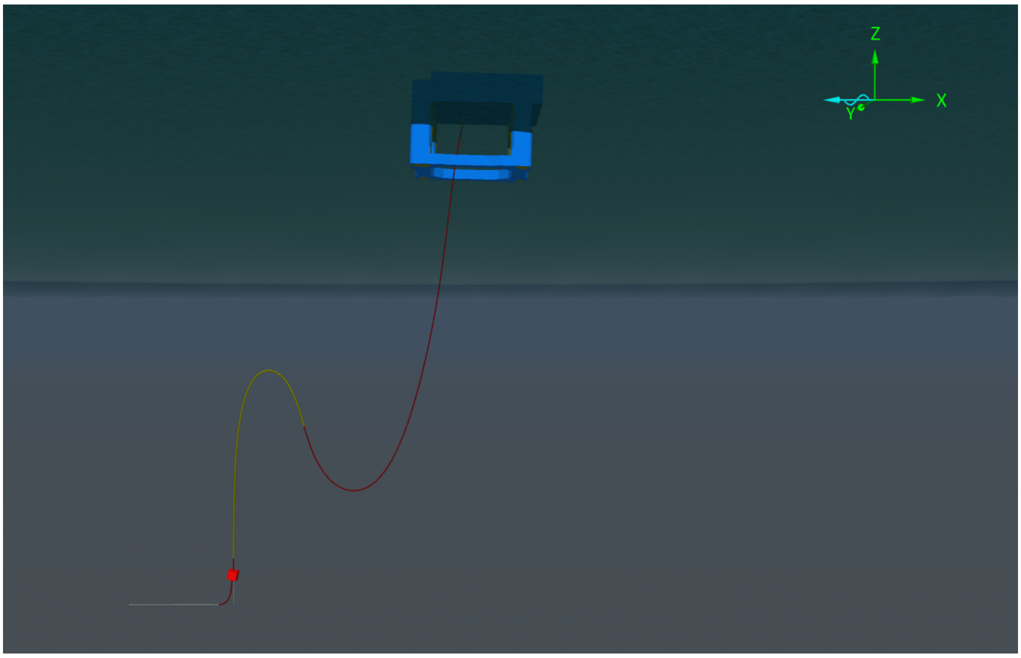


*Figure 18: Tether wave configuration, minimum bend radius in the buoyancy segment*

The tether remains in tension for all the analysed load cases. Figure 19 shows the tether at its minimum tension.

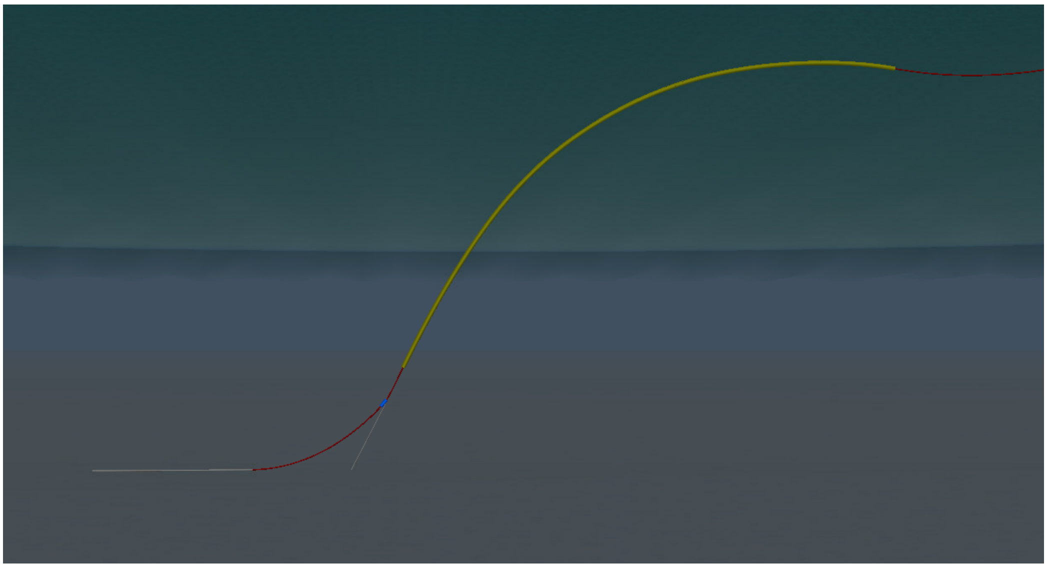

*Figure 19: Tether, minimum tension*

The maximum strain in the BS in the tether wave configuration remains below 10%, in compliance with the acceptance criteria. Figure 20 shows the maximum strain in % in the BS in static condition. Figure 21 shows the maximum strain, from all load cases, in % in the BS in dynamic condition.

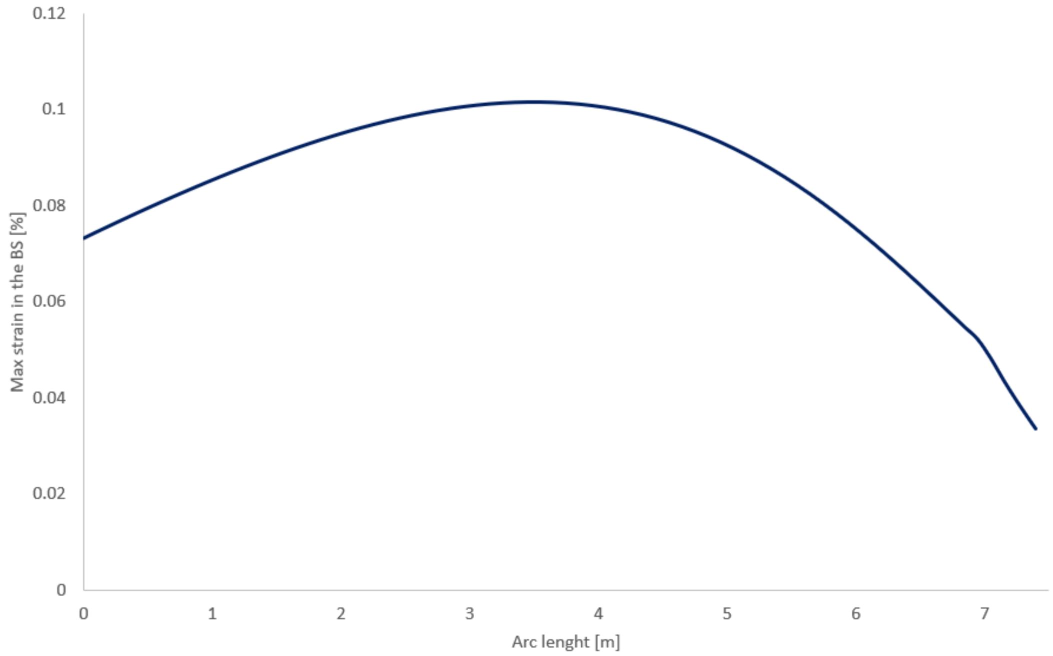


*Figure 20: maximum strain in BS [%], static*

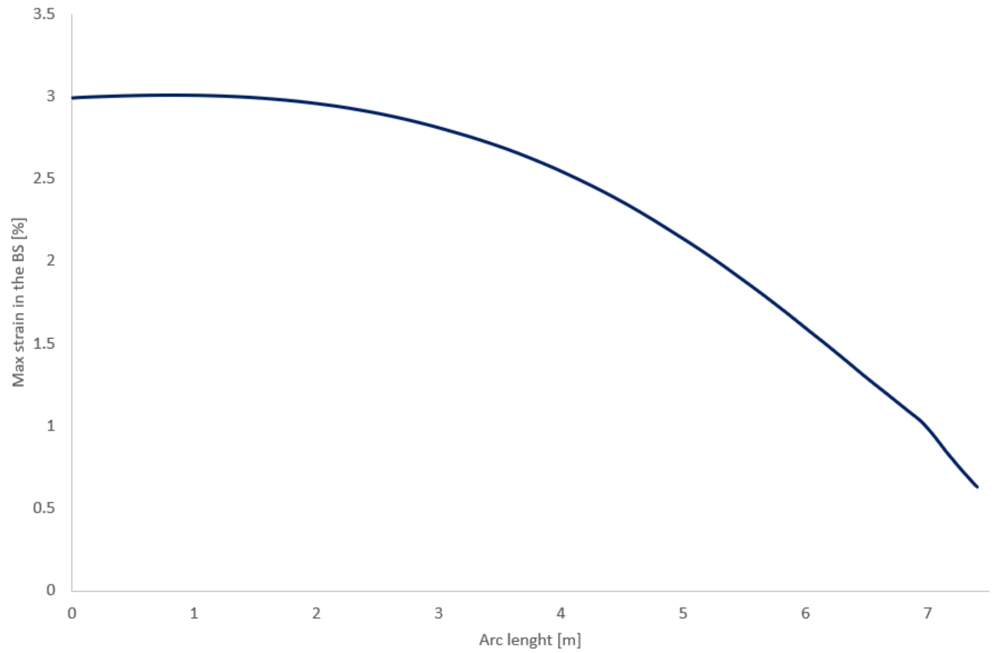


*Figure 21: maximum strain in BS [%], dynamic*

## 6.3 Fatigue Analysis Results

The fatigue analysis is studied for the lazy and tether wave configurations, in the BS area. The fatigue for the free-hanging case is not studied because the current configuration, cross-section and host are not able to provide a free-hanging dynamic cable that will fulfil the design criteria.

The design life is specified in 4.2. Table 13 confirms that the design life requirement is met for both lazy wave and tether wave configurations.

*Table 13: Design life for lazy wave and tether wave*

| Configuration | Environment | Design Life Fulfilled |
|---|---|---|
| Lazy wave | North Sea | Yes |
| Tether wave | North Sea | Yes |

## 6.4 Strain in the insulation

The outputs of the global analysis for the lazy and tether wave configurations are used to establish the strain in the internal cable components. In particular, the strain is calculated in the insulation part through a detailed analytical local analysis, based on literature ([2], [3]) and using Helica.

In particular, the tension and the curvature outputs from the global analysis are used to calculate the stress and the strain in the internal parts of the cable, as explained below.

It is assumed that the radial load applied by the outer layers of the cable (pressure applied by the extruded polymer sheaths and load applied by the armour wires under tension) is all transferred to the cable cores. This is a conservative assumption as in reality it will be shared between the cable cores and the plastic fillers.

The axial strain in the insulation, $\varepsilon_z$, in a helical component induced by axisymmetric loads and bending loads is the summation of three terms:

*Equation 1: axial strain*

$$\varepsilon_z = \varepsilon_A + \varepsilon_B + \varepsilon_f$$

Where $\varepsilon_A$ is the strain induced by the axisymmetric loads, $\varepsilon_B$ is the strain induced by the bending and $\varepsilon_f$ is the friction-induced axial strain.

The strain induced by the axisymmetric loads $\varepsilon_A$ considers tensions, torsion and pressure. The axisymmetrical analysis, studied with Helica, gives as output, the load sharing between the components of the cross-section and the contact forces between layers. $\varepsilon_A$ does not depend on the curvature, it only depends on the component tension.

Bending strain $\varepsilon_B$ occurs due to the curvature imposed on the cable during bending and its value increases linearly with the curvature. The bending strain, prior to slip, is calculated as shown in Equation 2.

*Equation 2: Bending strain prior to slip*

$$\varepsilon_B = \kappa_x \cdot [X_2 \cdot cos\alpha \cdot (1 + \sin^2 \alpha) \cdot \cos(\theta) + X_3 \cdot \cos^4 \alpha \cdot \sin(\theta)]$$

Where α is the lay-angle of the helical component, $\kappa_x$ is the global curvature with bending around the neutral axis, $X_2$ and $X_3$ are the local coordinates within the component and θ the angular coordinate in the cross section starting at the neutral axis. In this analysis, the outer diameter and $\theta$=90 degrees are considered.
As an assumption, the bending strain equation does not change after slip, leading to a simplified analysis. Consequently, a slightly larger bending strain is predicted after the slip.

The friction-induced axial strain, $\varepsilon_f$, is a function of the curvature $\kappa_x$ and at slip is given by Equation 3. The friction-induced strain increases with curvature until slip occurs, after which it stabilizes at a constant value.

*Equation 3: friction-induced axial strain at slip*

$$\varepsilon_f = \frac{R \cdot \theta}{E \cdot A \cdot \sin\alpha} \cdot f$$

Where E is the Youngs modulus, R is the helical radius, A is the cross-sectional area of the component and f is the available friction force per unit length of the helix component.
The critical curvature, $\kappa_c$, at which slip starts, is calculated as shown in Equation 4.

*Equation 4: critical curvature*

$$\kappa_c = \frac{f}{E \cdot A \cdot \cos^2\alpha \cdot \sin\alpha} \cdot \frac{\theta}{\sin\theta}$$

It is important to highlight the stick-slip behaviour for the calculation of the friction-induced strain as it influences the fatigue life of the cable. The strain-curvature graph consists of two regions: stick and slip. Initially, in the stick region, the cable starts bending without relative sliding between the layers, and then, as the curvature increases, there is a transition to 'slip' where increasing amount of relative sliding occurs between the element and adjacent layers.

To summarise, the curvature and the tension outputs from the global analysis are used to calculate the total strain. The strain is a summation of three terms, and the stick-slip behaviour is considered.

Figure 22 presents the dynamic strain range in the insulation for the lazy wave configuration in the BS area, and the y-axis is in logarithmic scale.

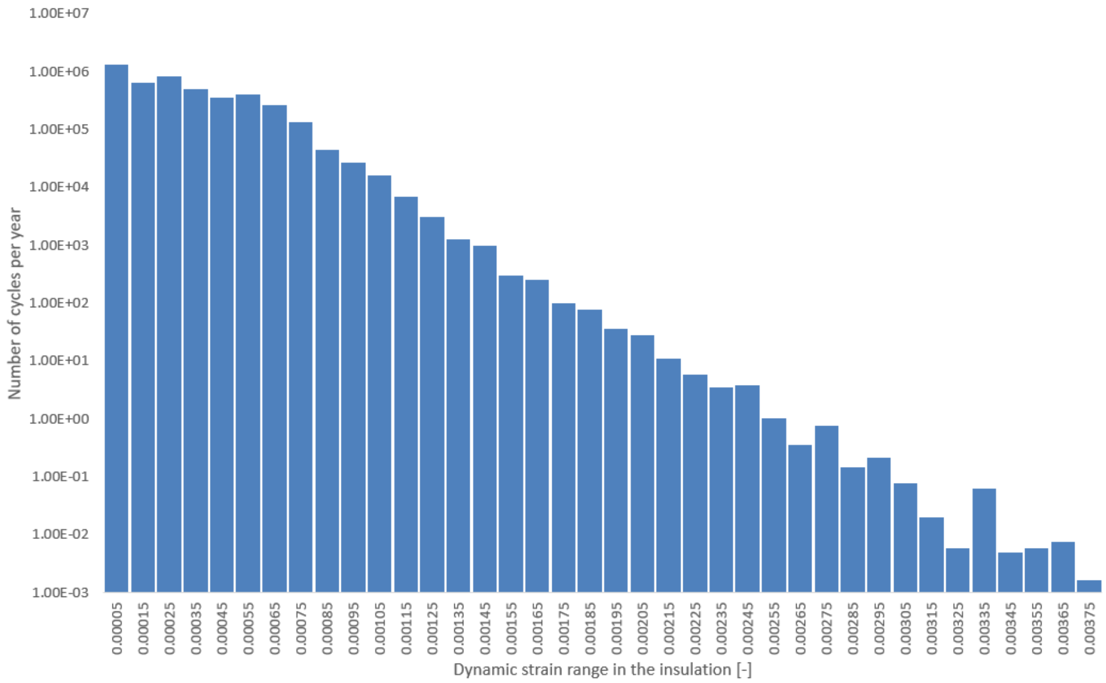


*Figure 22: Dynamic strain range in the insulation, lazy wave configuration, BS*

Figure 23 shows the dynamic strain range in the insulation for the tether wave configuration in the BS area, and the y-axis is in logarithmic scale.

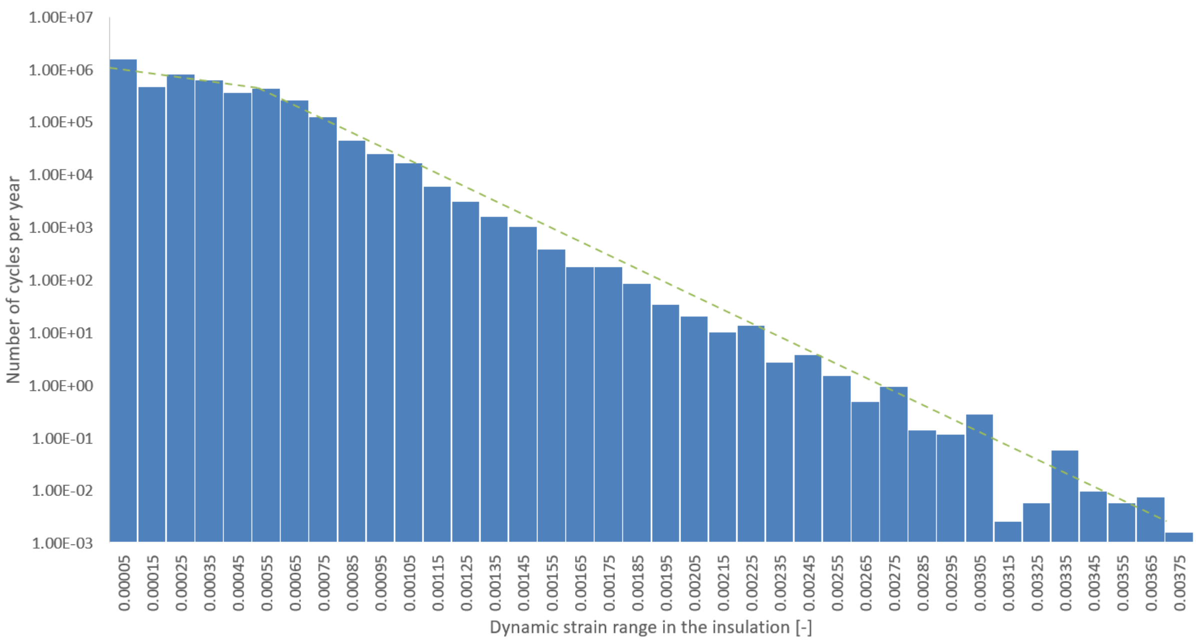


*Figure 23: Dynamic strain range in the insulation, tether wave configuration, BS*

The histograms highlight two distinct slopes (as highlighted by the green dashed lines in Figure 23): one corresponding to the presence of slip, and the other to its absence. The results show that the dynamic strain range in the insulation is always lower than 0.4%.

To identify the location of maximum strain along the entire cable length, the same analysis is performed on the sag-hog section. Figure 25 shows the dynamic strain range in the insulation for the tether wave configuration in the sag-hog area, and the y-axis is in logarithmic scale.

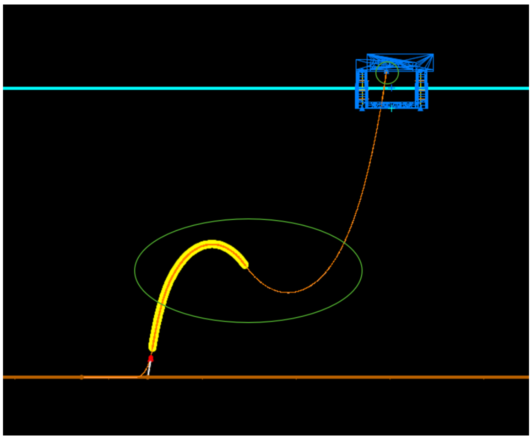

*Figure 24: BS and sag-hog areas, tether wave configuration*

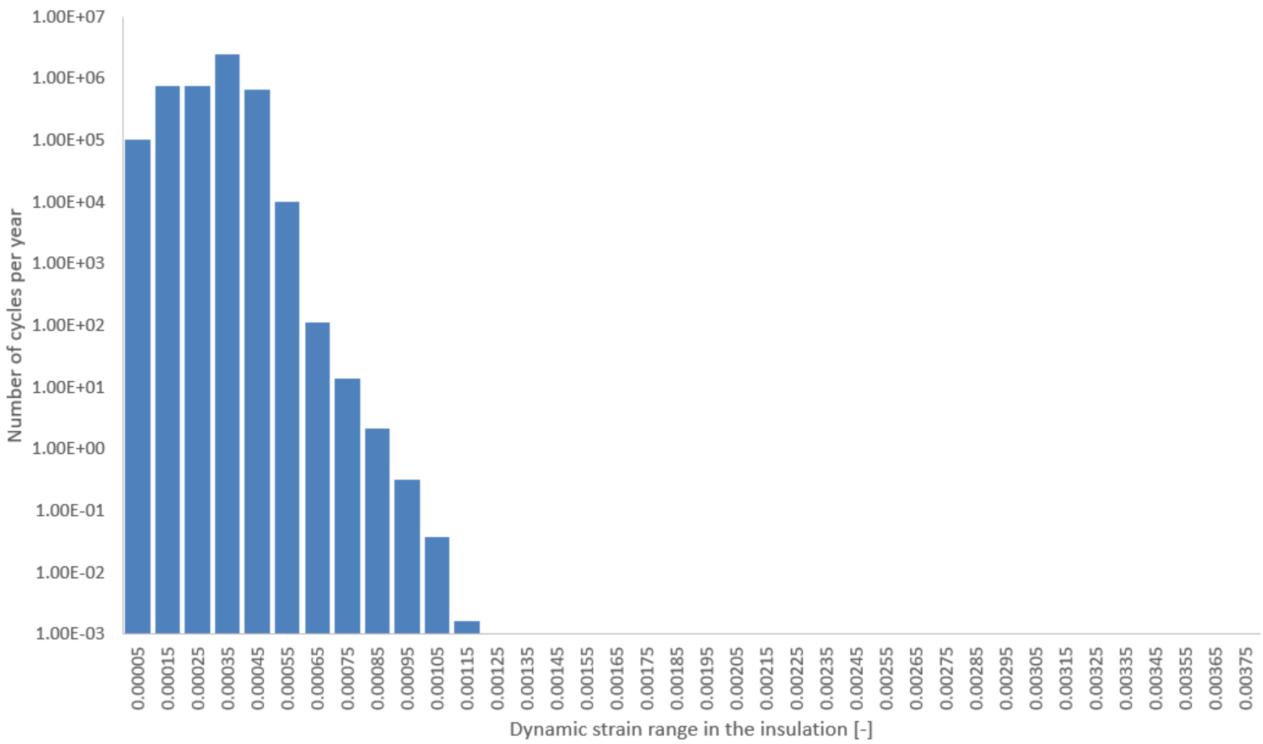


*Figure 25: Dynamic strain range in the insulation, tether wave configuration, sag-hog*

It is evident that the strain in the insulation in the sag-hog area of the cable is lower than before, around 0.1%, confirming that the critical area for the strain in the insulation is in the BS.

The same local analysis, including the calculation of the strain range in the insulation, is performed for extreme events corresponding to 100 YRP condition for the tether wave configuration. The analysis considers the maximum curvature occurring during extreme events along the entire length of the cable. The results indicate that the maximum strain range in the insulation is lower than 1.4%, across the full length of the cable, and below 0.8% within the bend stiffener region.

It should be emphasised that the previously presented data refers to the dynamic strain range. In addition, static strain due to assembly of the cores and strain due to extrusion must be considered. The static strain due to assembly of the cable cores does not exceed 1.5%. The strain due to extrusion process of the insulation can be studied in [4] .

## 6.5 Sensitivities

### 6.5.1 Alternative Hang-off Location

To introduce greater dynamic loads into the system, an alternative hang-off point, located at a larger distance from the platform centre, is investigated. Table 14 presents the alternative hang-off location in platform coordinate system.

*Table 14: Alternative hang-off location in platform coordinate system*

| X | Y | Z |
|---|---|---|
| -45.7 m | 2.25 m | 39.5 m |

Figure 26 and Figure 27 show the alternative hang-off location. Figure 28 shows the dynamic strain range in the insulation for the tether wave configuration in the BS area for the alternative hang-off location, and the y-axis is in logarithmic scale. Due to the greater dynamic, the design life is lower.

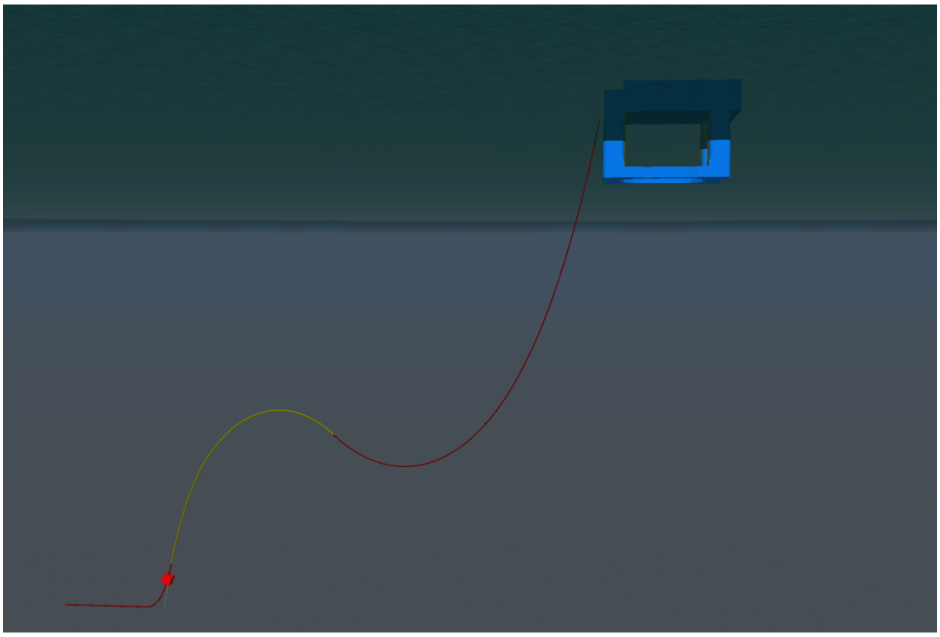

*Figure 26: Tether wave configuration, alternative hang-off location*

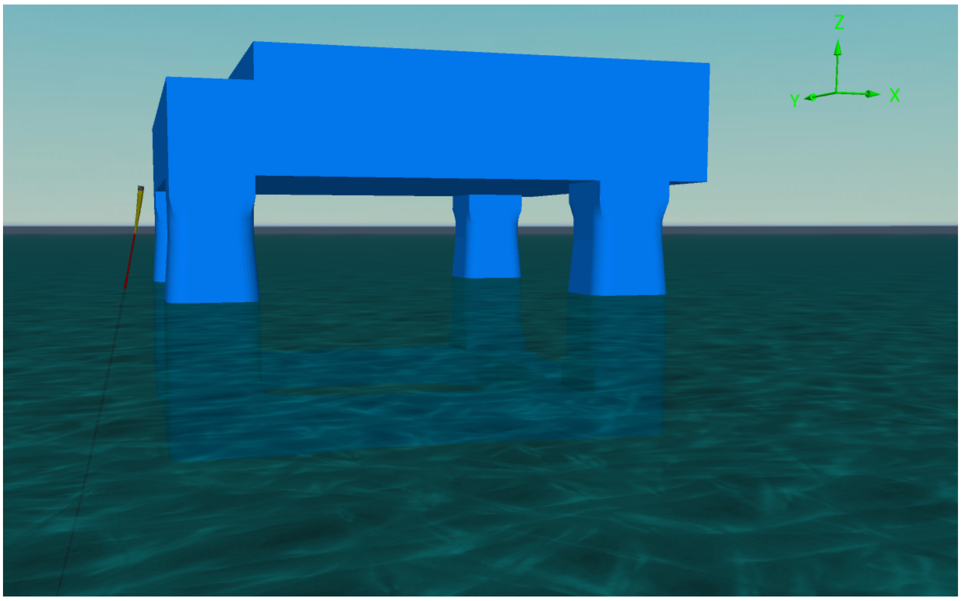


*Figure 27: Alternative hang-off location*

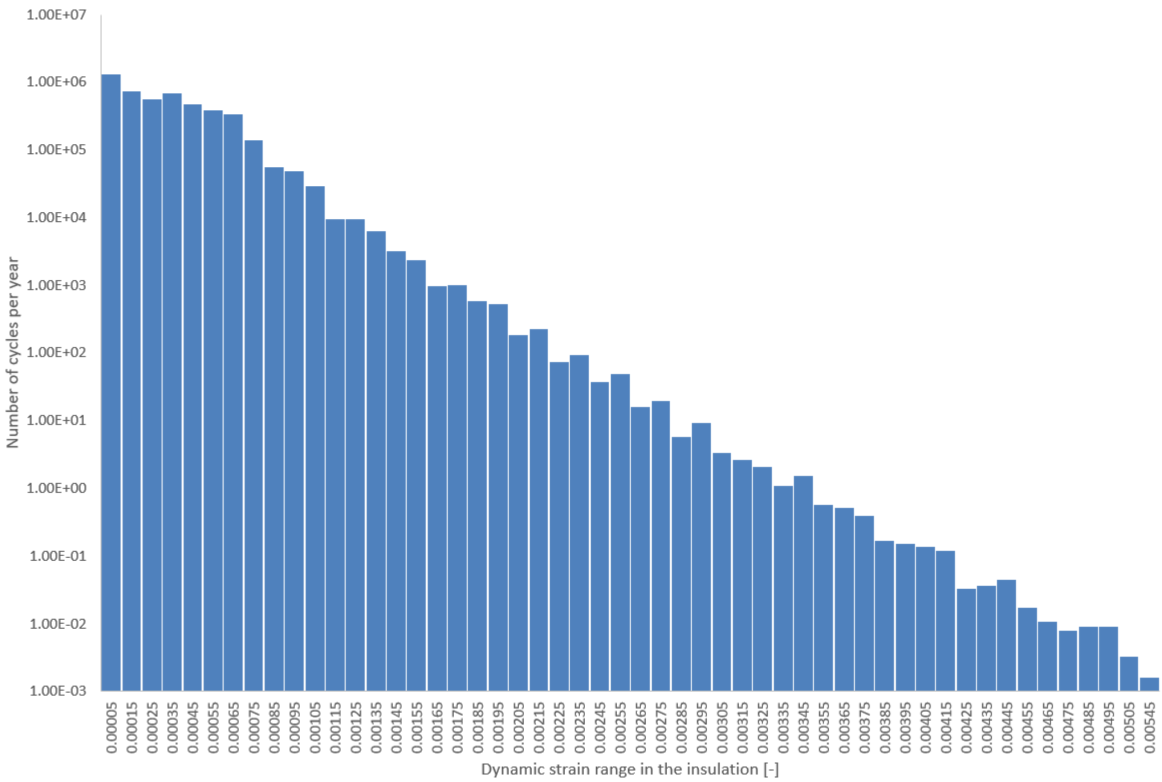


*Figure 28: Dynamic strain range in the insulation, tether wave configuration, alternative hang-off location*

For the worst hang-off location, resulting in very high dynamic loads, the maximum dynamic strain range is below 0.6%.

### 6.5.2 Full-stick Scenario

A full-stick scenario is considered in the analysis for a very conservative result. The strain is calculated under the assumption that the cable cores remain in full-stick, which leads to higher strain estimated values and lower fatigue life. Figure 29 shows the dynamic strain range in the insulation for the tether wave configuration in the BS area, and y-axis is in logarithmic scale.

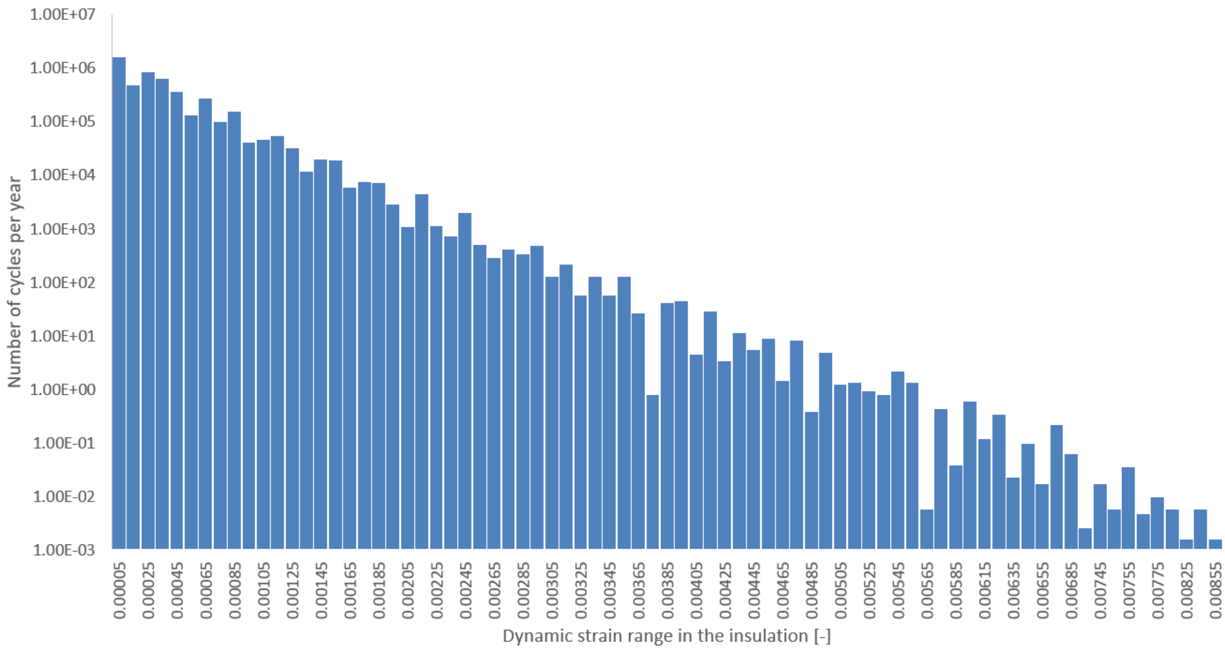


*Figure 29: Dynamic strain range in the insulation, tether wave configuration, full-stick scenario*

It is evident that the dynamic strain range is larger when calculated assuming full-stick. It is lower than 0.9%.

# 7 Conclusions

Extreme and fatigue analysis are studied in this report to establish realistic loads and strains in a dynamic HVDC export cable located in the North Sea and connected to a floating substation. The results from the extreme analysis show that the 1.4 GW ±320kV HVDC FOSS by Aibel AS and Hitachi Energy exhibits very good motion characteristics for the North Sea environments. Lazy and tether wave configurations for high-voltage DC dynamic cables constitute real project options and the fatigue analysis demonstrates that the design lifetime of the cable is fulfilled. Although free-hanging is not found to be fit for purpose under these environmental conditions, platform type, offsets and cable design, it can be a viable solution in locations with more benign environmental conditions.

The local analysis of the cable in the insulation component shows that the maximum dynamic strain range seen during an extreme event corresponding to 100 YRP is lower than 1.4% considering the entire length of the cable. The fatigue analysis during 30 years of operation shows that the typical fatigue loads are lower. The dynamic strain ranges in the insulation are always lower than 0.4%, considering the proposed hang-off location for the platform and stick-slip behaviour.

The results confirm that the dynamic strain level in fatigue loading used in [5] is realistic for typical applications in the North Sea. Specifically, it was tested and stated that the bending strain varies between 0% and 1%, in accordance with the results of this analysis. However, in extreme events 100 YRP the dynamic strain can be higher.

# 8 Bibliography


[1] "NORSOK STANDARD N-003 Actions and action effects," 2007.

[2] D. D. Tjahjanto, A. Tyrberg and J. Mullins, "BENDING MECHANICS OF CABLE CORES AND FILLERS IN A DYNAMIC," OMAE, 2017.

[3] G. Skeie, N. Sødahl and O. Steinkjer, "Efficient fatigue analysis of the helix elements in umbilicals and flexible risers: Theory and applications," 2012.

[4] N. H. C. Gustaf Larsson, "Stress prediction of high voltage XLPE cable insulation system with regard to water tree ageing".

[5] SINTEF, NTNU, E. R&D, Borealis, N. Norway, Statkraft, Statnett and Statoil, "Water Tree Ageing of High Voltage XLPE Cable Insulation System under Combined Dynamic Mechanical and AC Electrical Stress," CIGRE, 2014.

[6] DNV, "DNV-RP-C205 Environmental conditions and environmental loads," April 2025.

# Deliverable 2.1

## Mechanical load profiles

Project funded by

Schweizerische Eidgenossenschaft
Confédération suisse
Confederazione Svizzera
Confederaziun svizra
Swiss Confederation

Federal Department of Economic Affairs, Education and Research EAER
State Secretariat for Education, Research and Innovation SERI

Co-funded by the European Union

DC DYNAMIC

# Deliverable 2.1

## Mechanical load profiles

**NKT**

**Andreas Tyrberg,**
**Alessio Rubini,**
**Nikolaos Psichogios,**
**Angelica Chisté**

DC DYNAMIC

Project funded by
Schweizerische Eidgenossenschaft
Confédération suisse
Confederazione Svizzera
Confederaziun svizra
Swiss Confederation
Federal Department of Economic Affairs, Education and Research EAER
**State Secretariat for Education, Research and Innovation SERI**

Co-funded by the European Union